Journal of Atmospheric and Solar-Terrestrial Physics 72 (2010) 913–925

Contents lists available at ScienceDirect

Journal of Atmospheric and Solar-Terrestrial Physics

journal homepage: www.elsevier.com/locate/jastp

Attempts to create ball lightning with triggered lightning

Jonathan D. Hill, Martin A. Uman*, Michael Stapleton, Douglas M. Jordan, Alexander M. Chebaro, Christopher J. Biagi

Department of Electrical and Computer Engineering, University of Florida, Gainesville, FL 32611, USA

ARTICLE INFO

Article history:
Received 30 October 2009
Received in revised form
31 March 2010
Accepted 12 April 2010
Available online 12 May 2010

Keywords:
Ball lightning
Lightning
Atmospheric electricity
Triggered lightning
Electrical discharges

ABSTRACT

We describe attempts to create ball lightning by directing lightning, triggered from natural thunderclouds using the rocket-and-wire technique, through a variety of materials. Some of the observed phenomena have features in common with natural ball lightning or with laboratory attempts to create it: flame-like luminosity for up to 0.5 s above salt water; constant-luminosity silicon fragments falling for about 1 s under the influence of gravity; a 0.7 m region of stationary luminosity whose bottom was 0.3 m above a stainless steel surface to which arcing had occurred; and a glow for about 0.5 s above pine tree sections.

1. Introduction

The experiments reported here were motivated by two classes of recent ball-lightning-related laboratory experiments and a recent theory of the formation of ball lightning. In the recent theory, Abrahamson and Dinnis (2000) and Abrahamson (2002) view ball lightning as being formed from silicon originally resident in sand (SiO_2) and released by a lightning strike and associated chemistry to form silicon "webs" that oxidize, emitting light. The two classes of experiments are (1) those of Paiva et al. (2007) and Stephan and Massey (2008) in which electric arcs terminating on solid silicon and other pure metals produced small luminous metal spheres, apparently not dissimilar from phenomena that can occur in arc welding (Hu and Tsai, 2006) and (2) those of Versteegh et al. (2008) and earlier similar experiments referenced in that work in which luminous, flame-like structures were generated above the surface of water volumes (tap water or distilled water containing calcium, lithium, or copper salt additives) through which electric arcs were passed.

Ball lightning is a phenomenon for which there exist numerous eye-witness reports but little, if any, verifiable scientific documentation such as photographs or video records (Stenhoff, 1999; Rakov and Uman, 2003). Despite the lack of such documentation, the properties of ball lightning are relatively well accepted from statistical analyses of observers' reports spanning a period of three centuries. There are at least nine significant compilations of eyewitness observations of ball lightning, containing almost 5000 reports (Stenhoff, 1999; Rakov and Uman, 2003). More than one type of ball lightning may well have been observed, and hence there may be multiple mechanisms by which the generic phenomenon known as ball lightning is generated. Detailed statistics on size, color, duration, and other reported properties of ball lightning are found in Stenhoff (1999) and Rakov and Uman (2003) and are briefly reviewed below. The most commonly reported observation is of an orange-to-grapefruit-size sphere (the range for the vast majority of reports is from the size of a golf ball to that of a basketball), which is usually red, orange, or yellow in color with luminosity about as bright as a 60 W light bulb. Ball lightning is most often reported to have a duration of a few seconds, during which time it generally moves more or less horizontally (it does not rise as would hot air) and then decays either slowly and silently or abruptly and explosively. The luminosity of ball lightning is reported to be roughly constant until it extinguishes. It is most often seen spatially close to and just after the occurrence of a cloud-to-ground lightning flash. It has been reported to pass through glass windows and metal window screens. There are a significant number of credible reports of ball lightning occurring within metal (aluminum) aircraft, both commercial and military. Ball lightning has been reported to have been generated from high-power electrical equipment such as battery-bank switches. Ball lightning is sometimes reported to have an odor and sometimes to leave burn marks. Human beings are seldom, if ever, injured or killed by ball lightning. Most reports of injury and death are from the 18th and 19th centuries and can

* Corresponding author. Tel.: +1 352 392 4038; fax: +1 352 846 3363.
E-mail address: uman@ece.ufl.edu (M.A. Uman).

1364-6826/$ - see front matter © 2010 Elsevier Ltd. All rights reserved.
doi:10.1016/j.jastp.2010.04.009

probably be attributed to ordinary lightning or to meteors. Ball lightning and meteors are both referred to in the literature from that time period as "fireballs".

There have been many theories devised to explain ball lightning. These are reviewed by Stenhoff (1999) and Rakov and Uman (2003). No theory is completely satisfactory, most simulate only a limited number of the observed characteristics of ball lightning, and some are particularly suspect (e.g., electron–positron annihilation, miniature black holes, cosmic rays focused by cloud electric fields, quantum mechanical plasmas). Ball lightning models can generally be divided into two classes: those that are internally powered (e.g., by on-going chemical reactions) and those that are externally powered (e.g., from the steady ambient electric fields of clouds). It is arguable whether ball lightning has been produced in the laboratory. Nevertheless, many luminous phenomena created in the laboratory are claimed by their creators to be ball lightning or to have some relation to ball lightning. Most recently, Stephan and Massey (2008) have credibly argued that the 0.1–1.0 mm molten-metal luminous spheres they produced in the laboratory might be considered to be one class of naturally observed ball lightning.

The research described here involves artificially initiating (triggering) lightning from natural thunderstorms using the rocket-and-wire technique (e.g., Uman et al., 1997; Rakov, 1999; Rakov and Uman, 2003) and directing the lightning current through a variety of different materials in an attempt to create ball lightning. In this study, we triggered 8 lightning flashes to a total of about 100 samples of liquid, solid, and powdered material, both organic and inorganic. We do not claim to have created ball lightning. The observation deemed to be most similar to natural ball lightning occurred on September 17, 2008 and is described in detail in Section 3. In this case the lightning current was directed across a 10 cm gap between a vertical steel rod and a horizontal, wet, stainless steel plate beneath, both supported by a wood frame. A well-defined persistent glow appeared around and above the stainless steel plate and then separated from the plate and hovered above it, unaffected by the subsequent lightning current variations. The separated glow, initially about 71 cm wide and 48 cm high with its lower edge being about 30 cm above the stainless steel plate, had a total duration of 266 ms. In other experiments, we reproduced and will describe in Section 3, the laboratory experiments discussed in the first paragraph above: by way of lightning current directed (1) through silicon disks and (2) through pools of salt water, we generated (1) small glowing metal spheres of relatively constant luminosity with a duration exceeding 1 s that fell under the influence of gravity and (2) luminous rising flames of up to about 0.5 s duration that appeared above the surface of the salt water through which lightning current was passed.

2. Background and experimental setup

Fig. 1 shows the rocket launching facility at the International Center for Lightning Research and Testing (ICLRT) located at the

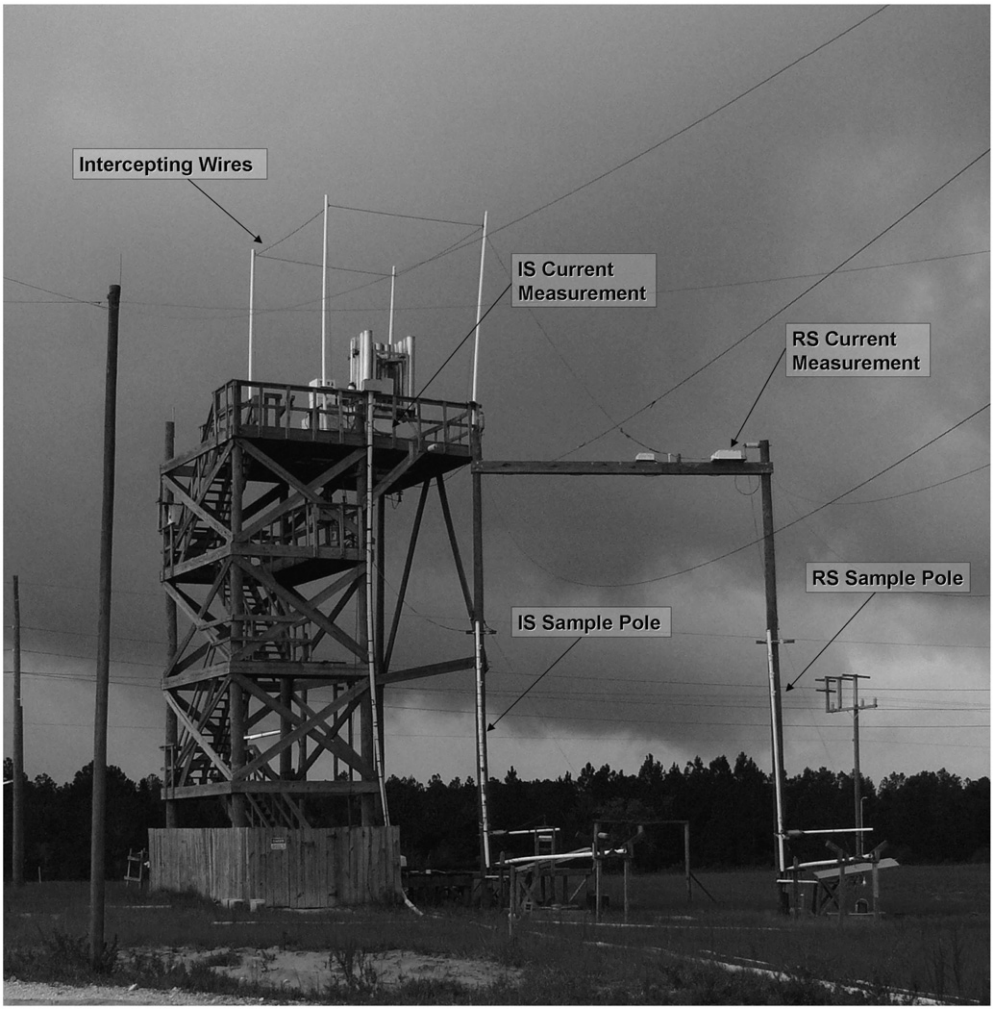

Fig. 1. Tower for launching rockets trailing grounded wires for triggering lightning, along with ball lightning experimental setup, as viewed looking southwest.

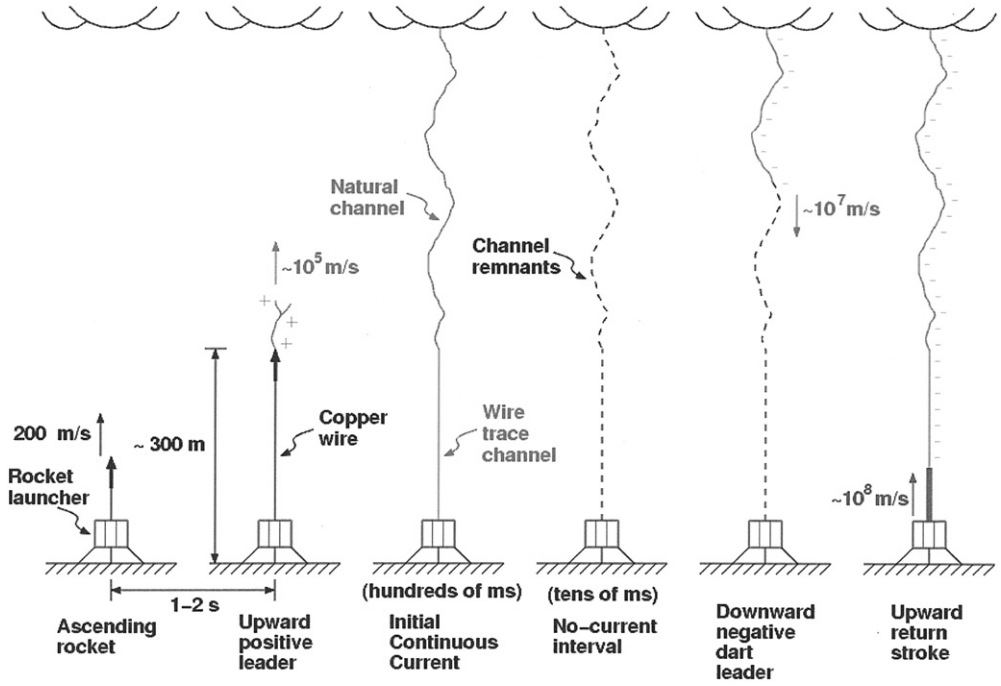

Fig. 2. Sequence of events occurring in classical rocket-and-wire triggered lightning. The Upward Positive Leader and Initial Continuous Current constitute the Initial Stage (IS) process.

Camp Blanding Army National Guard Base in north-central Florida. The launching facility is shown outfitted for the ball lightning experiments that took place during Summer 2008. Rockets trailing grounded, kevlar-coated copper wires were launched from the aluminum launching tubes located on the top of the 11 m wood tower. A drawing illustrating the general mechanisms of the rocket-and-wire triggering of lightning is found in Fig. 2. The current at the base of a typical triggered lightning can be considered to be composed of two distinct phases. The first phase is termed the Initial Stage (IS) which involves the current of an upward positive leader (UPL) followed by an Initial Continuing Current (ICC). The UPL is initiated from the tip of the ascending triggering wire (typically at an altitude of 100–300 m), and the subsequent connection of the UPL with the cloud charge overhead (at perhaps 7 km) leads to the ICC. The IS current is relatively low in amplitude, from less than a hundred amperes to several thousand amperes, with a total duration of some hundreds of milliseconds. Following the UPL current and the ICC, during which the triggering wire is destroyed (typically about 10 ms after the initiation of the UPL), the second phase of the triggered lightning may or may not occur. That phase consists of one or more downward-moving dart-leader/upward-moving return stroke sequences that traverse the remains of the channel left by the ICC following a period of typically some tens of milliseconds during which no current flows. Return stroke (RS) currents exhibit rise times of a microsecond or less and typical peak amplitudes of 10–15 kA. Return strokes are sometimes followed by "continuing currents" of hundreds of amperes with durations of tens to hundreds of milliseconds. These continuing currents are not unlike the ICC.

A still photograph (6 s time exposure) of lightning triggered to the launch tower is given in Fig. 3. Wind blowing to the right separates the illuminated wire (straight luminous channel on the left and its debris to the right) from the five dart-leader/return stroke sequences blown further to the right.

During the rocket-triggered lightning/ball lightning study, two different physical configurations were employed to direct the lightning current through the various material samples. The final setup (shown in Fig. 1), is discussed in the next paragraph. The initial setup involved a single, common path to ground for both IS

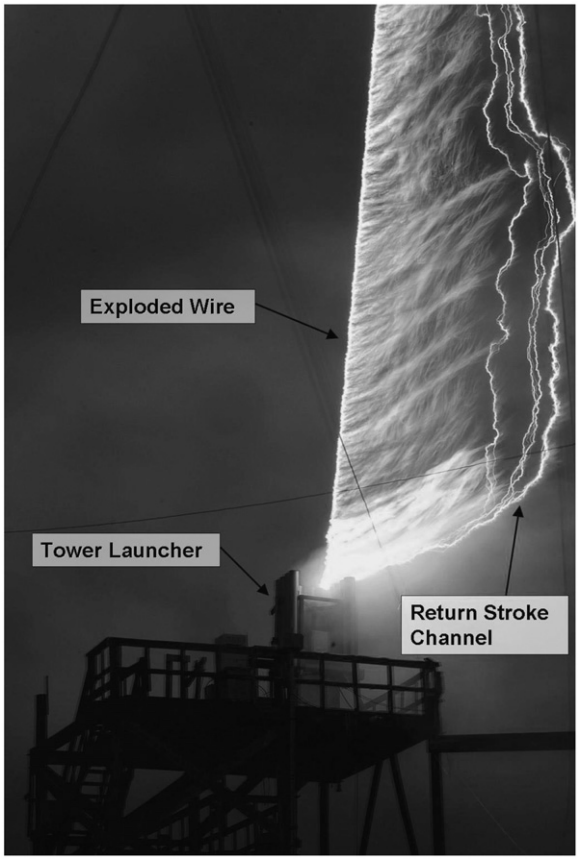

Fig. 3. Rocket-and-wire triggered lightning (6 s exposure).

and RS currents. A non-inductive T&M Research R-7000-10 Current Viewing Resistor (shunt) was used to measure the current beneath the tower launcher. The shunt has an internal resistance of 0.001 Ω and a bandwidth of 8 MHz. Current waveform data were transmitted via Opticomm fiber-optic links from the shunt on the tower to the Launch Control trailer, located about 50 m to the north. There the analog data were digitized by Yokogawa and LeCroy oscilloscopes. A 6 m section of 10 cm diameter PVC was outfitted with standoffs that supported sections of copper braided wire carrying the lightning current. Spark gaps were positioned along the braided wire where material samples could be inserted for exposure to the lightning current. The bottom of the braided wire was connected to a copper rod whose lower end was positioned underwater in the center of a 2 m diameter swimming pool filled with salt water. Braided wire was fastened to the inner circumference of the swimming pool under water and grounded to the launch tower grounding system. An approximately 1 m radial spark gap was thereby created under water between the bottom of the copper rod and the outer edge of the swimming pool.

The final experimental configuration for the ball lightning experiment is shown in Figs. 1 and 4. The intent of this configuration was to separate spatially the two current components, IS and RS, of the triggered lightning. This was accomplished by installing a rectangular intercepting wire (Fig. 1) over the top of the tower launcher. While the IS current flowed through the tower launcher on a path to ground via the same shunt as in the initial measurement setup, after the vaporization of the triggering wire and the termination of the ICC, dart-leader/return stroke sequences generally attached to the intercepting wire above the tower launcher. From the intercepting wire the RS current was diverted along a separate path to a second current measurement located on top of a second telephone pole installed approximately 7.5 m west of the first configuration's support pole. A non-inductive T&M Research R-5600-8 Current Viewing Resistor (shunt) was used to measure the RS current. The shunt has an internal resistance of 0.00125 Ω and a 12 MHz bandwidth. Like the IS measurement, RS current waveforms were transmitted to the Launch Control trailer via Opticomm fiber-optic links and digitized in the Launch Control trailer. Fig. 4 shows triggered lightning illuminating samples suspended from both IS and RS PVC sample poles and also illuminating the salt water in the child's swimming pool at the bottom of the RS pole. Fig. 5 shows a close-up view of the swimming pool. Fig. 6 shows an example of two suspended silicon wafers through which lightning current had passed via an arc gap. Material samples were either suspending freely in the air as in Fig. 6 or contained in small vertical PVC tubes of 10 cm height and 1.5 cm diameter with side openings of around 175 mm^2 to the outside air.

Fig. 4. Six second exposure showing exploded material samples on both the IS (furthest) and RS (closest) sample poles and the swimming pool flame (foreground), as viewed looking southeast.

Photographic data from the ball lightning experiment were acquired by a Phantom v7.0 High-Speed camera, four Sony HDR-HC5 high-definition video cameras, and four Nikon N2000 35 mm SLR cameras. The Phantom camera was operated from the Launch Control trailer, located, as noted earlier, 50 m north of the launch tower. The Phantom camera acquired data at a frame rate of 500 frames/s (2 ms resolution) and was triggered at the time of the rocket launch. A Sony HD camera and Nikon 35 mm SLR also recorded the same field of view from the Launch Control trailer. In addition, Sony HD cameras and additional 35 mm SLR cameras were placed in other structures around the ICLRT. Each 35 mm camera took a 6 s time-exposure after being activated at the time of the rocket launch. Two stacked ND4 neutral-density filters were used on all 35 mm cameras to prevent over-exposure.

There were a total of eight successful triggered lightning events during the ball lightning experiment, four with both IS and RS currents and four with only IS currents. Table 1 provides general background information on all eight events including the launch time, peak current, number of strokes, and the quasi-static electric field at ground when the rocket was launched. Rocket triggered lightning events are designated by UF-08XX where the last two numerical digits correspond to the shot number of the calendar year. The triggered lightning event on June 10, 2008 was the only attempt to create ball lightning with both the IS and RS currents routed through the material samples on a common path to ground (the initial configuration). All events after June 10, 2008 use the intercepting wire described above and shown in Fig. 1 to divert the RS current to a separate string of material samples. A complete listing of all material samples tested during the ball lightning experiment is found in the Appendix. A significant fraction of the samples tested were suggested by scientists interested in ball lightning whom we informed in advance of the experiments. Samples ranged from fresh bat guano to powered carbon and powdered metals (with and without additives such as sulfur, KNO_3, and water) to salt water to sections of pine trees. In the Appendix, material samples are listed for both the IS and RS sample poles (when applicable) in order of descending height placement on the two poles. For most cases similar material samples were mounted on both the IS and RS sample poles in order to determine whether long duration/low amplitude or impulsive/high amplitude currents were more likely to produce ball lightning or ball-lightning-like effects.

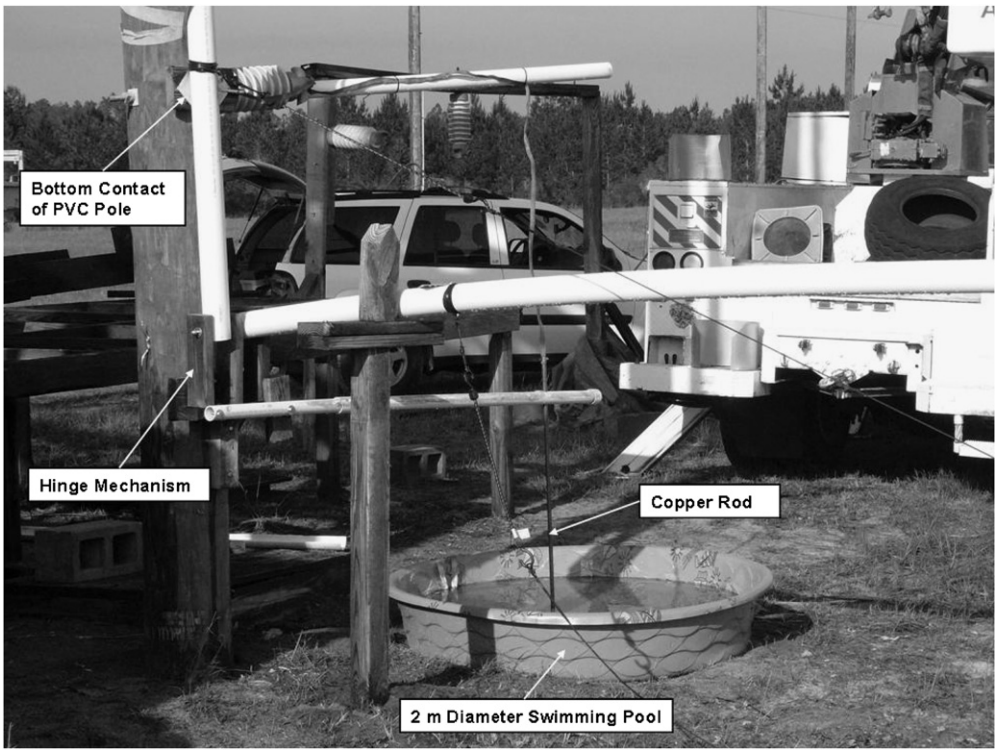

Fig. 5. Base of PVC pole, copper rod, and grounded swimming pool.

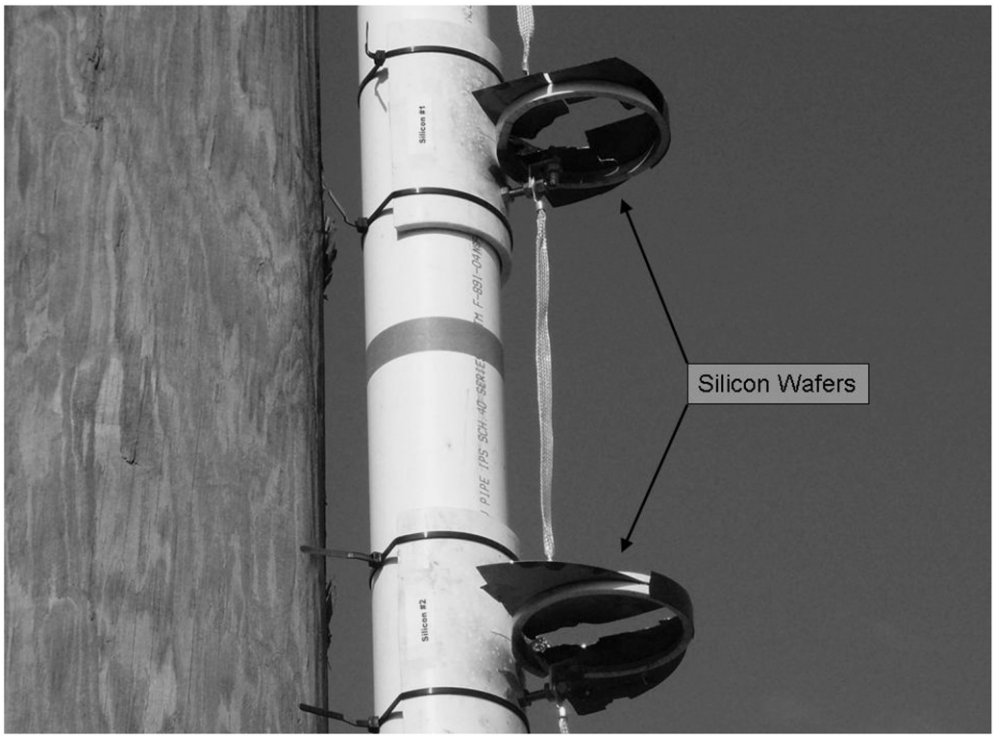

Fig. 6. Lightning-damaged silicon wafers.

3. Results and discussion

Of the eight triggered lightning events, only two produced photographic data we consider interesting in the context of ball lightning. All other material ignition produced luminous durations significantly less than about 300 ms and/or had other characteristics inconsistent with ball lightning. No events with sustained luminosity exceeding 100 ms were observed as a result of RS currents. All luminous phenomena which might be considered related to ball lightning were produced by lightning currents of the order of 100 A with durations of the order of 100 ms. The discussion to follow will be primarily concerned with the results of the flashes triggered on 6/10/08 and 9/17/08: on 6/10/08 (UF 08-02), (event A.1 below), a "flame" in/above the

Table 1
Triggered lightning events during the ball lightning experiment.

Shot	Date	Launch time (UT)	Result	Peak RS current (kA)	Number of strokes	E-field (kV/m)
UF 08-02	6/10/08	19:32:00	IS and RS	24	6	−5.5
UF 08-04	6/29/08	21:36:29	IS	–	–	−5.2
UF 08-08	6/30/08	18:41:24	IS and RS	18	5	−5.7
UF 08-11	7/12/08	17:52:49	IS and RS	17	3	−5.9
UF 08-12	7/23/08	18:40:21	IS	–	–	−5.8
UF 08-13	7/27/08	20:22:21	IS	–	–	−6.2
UF 08-17	9/11/08	20:36:56	IS	–	–	−5.3
UF 08-18	9/17/08	22:04:15	IS and RS	21	9	−6.3

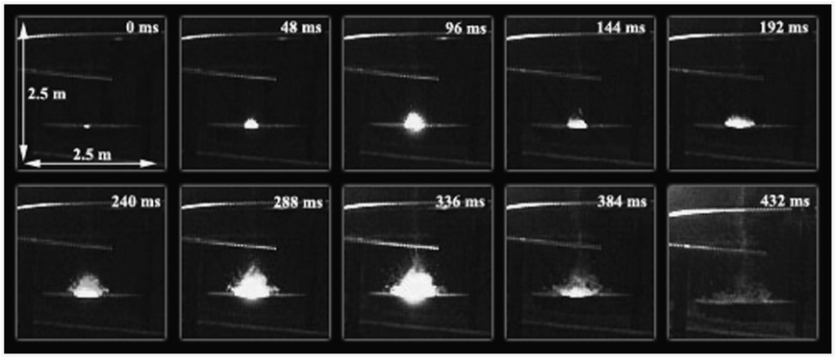

Fig. 7. Extracted frames of the swimming pool flame during the ICC process of UF 08-02 starting 80 ms after the full ignition of the triggering wire.

swimming pool filled with salt water, and (A.2), falling, glowing silicon particles; on 9/17/08 (UF 08-18), (B.1), a well-defined persistent glow above a stainless steel surface (of all the luminous phenomena produced, this event most resembled natural ball lightning) and (B.2), a persistent glow above a pine tree trunk mounted in a swimming pool filled with salt water.

We discuss now the four events (A.1, A.2, B.1, B.2) noted above.

Event A.1: Triggered lightning flash UF 08-02 was an unusual one in that a full seven seconds elapsed between the rocket launch and the initiation of the UPL, whereas several seconds is more typical. The triggering wire had likely unfurled to its full 700 m and was falling at the time of flash initiation. The IS current for UF 08-02 was relatively long in duration, between 700 and 800 ms with a charge transfer greater than 60 C. Arcs are seen on the material samples placed on the PVC pole approximately 90 ms prior to the full ignition of the triggering wire. The first visible arc in a salt-water-filled swimming pool (similar to that shown in Fig. 5) at the bottom of the single down-conductor occurred about 80 ms after the full ignition of the triggering wire. A "flame" appeared above the water surface in the swimming pool at this point and persisted for 432 ms. An average current of the order of 100 A flowed during the full duration of the flame. The flame generally expanded upward and outward in size during this time and peaked in luminous intensity during sequences of pulses (so-called ICC pulses) superimposed on the more steady ICC. The ICC pulses have durations to several milliseconds and current amplitudes to the thousand ampere range. Interestingly, the ICC continued for another 230 ms after the flame extinguished. No arcs appeared above the water surface during this time interval. The flame reached a maximum width of approximately 1 m. Fig. 7 shows a sequence of ten cropped frames extracted from the Phantom video at 48 ms intervals during the ICC process spanning the total 432 ms that luminous phenomena were evident above the water surface. The first frame corresponds to the initial arc seen in the swimming pool 80 ms after the full ignition of the triggering wire.

Following the ICC and after the first return stroke (peak current 21 kA), a new flame persisted above the water surface in the swimming pool for a time of 46 ms. There were 26 ms of continuing current following the return stroke before an M-component (similar to an ICC pulse and superimposed on the continuing current) occurred 28 ms after the first stroke. The flame extinguished approximately 18 ms after the M-component. The second return stroke (peak current 8 kA) occurred 132 ms after the first stroke producing a flame above the pool with a duration of only 6 ms. The third return stroke (24 kA) occurred 162 ms after the first stroke, and was followed 10 ms later by the fourth return stroke (4.4 kA). The continuing current duration following the third stroke was approximately 47 ms. Luminosity persisted above the swimming pool for 90 ms following the third stroke. The fifth return stroke (16.3 kA) occurred 274 ms after the first stroke and was followed by the sixth return stroke (3.7 kA) 8 ms later. The flame in the pool had a duration of 4 ms following the fifth stroke and only 2 ms following the sixth stroke. Neither the second, fifth, or sixth stroke had any appreciable continuing current. From these observations, it appears that there is a strong correlation between the lifetime of the flame above the swimming pool and the presence of slowly varying, relatively long-duration current flow (due either to the IS process or to continuing current following a return stroke). Similar flames above the salt-water pool on both the ICC and RS paths in the final configuration were seen on 6/30/08 (UF 08-08) and 7/12/08 (UF 08-11).

Event A.2: A second event of interest occurred during UF 08-02 and resulted from the explosion of two silicon wafers (see Fig. 6 and the detailed material description in the Appendix). The first silicon particles appear to erupt from the wafers approximately 212 ms after the full ignition of the triggering wire. However, the primary silicon particle shower did not begin until 520 ms after the triggering wire fully ignited. The full duration of the silicon particle shower was approximately 3.35 s. The lightning current ends approximately 580 ms after the first silicon particles erupt from the wafers. Most individual particles appeared to strike the

ground between 0.75 and 1.25 s after being emitted from the lightning-struck silicon wafers. Most particles demonstrated relatively constant luminosity as they fell, and they fell with more-or-less constant acceleration. A video was created showing the luminosity from the falling silicon particles integrated over the full particle shower. The final frame from the video is shown in Fig. 8 from which it is evident that the falling particles retained a relatively constant luminosity for a second or more, characteristics commonly reported for ball lightning. Falling under the influence of gravity is not a commonly observed ball lightning characteristic, although the literature does contain accounts of ground-based rolling balls and balls that bounce on hitting ground. Additionally, individual particles are seen to deflect when they struck the structures below them and to bounce when they impacted the ground. Attempts were made to measure the sizes of various falling silicon particles from the Phantom video records. Most of the particles were smaller than two pixels (around 8 cm^2) in area. Given this poor resolution and the presence of video blooming effects, the silicon particles were likely smaller than 4 cm^2 in cross-section. According to Stephan and Massey (2008) the glowing metal spheres they produced in the laboratory were in the 0.1–1 mm diameter range, but would be perceived as larger from either normal photography or by the human eye (see Section 5).

Event B.1: UF 08-18 was a nine-stroke flash with peak return stroke current of 21 kA. The IS and RS currents flowed down different paths to ground. No material samples were placed on either the IS or RS PVC poles, and twelve gauge solid core copper wire was used to short-circuit the spark gaps on both poles. The IS current was routed to a galvanized-steel rod electrode mounted vertically and about 10 cm above the top plane of two stacked 304 stainless steel plates, as shown in Fig. 9. The top stainless plate was about 1.3 cm thick and the bottom stainless plate was about 3.8 cm thick. Both plates were square with a side length of 30 cm. The two stainless plates were in pressure contact and were also connected together by a piece of braided wire. A second galvanized-steel metal rod electrode was mounted under the bottom stainless plate with a spark gap of approximately 7.6 cm. The locations of the 304 stainless plates, foreground PVC pipe, and top electrode are marked in Fig. 9 for height reference. The PVC pipe in the foreground of Fig. 9 is at approximately the same height as the top of the wood stand, but the camera perspective makes the PVC pipe appear higher. The top rod electrode passes through about 23 cm of the wood support structure. Beneath the electrodes and stainless steel plates, the IS current was directed to a pine tree trunk, as discussed in B.2 below. The experiment involving the stainless steel plates was not originally intended to be part of the ball lightning study, but rather was part of a different experiment to measure the surface damage to stainless steel as a function of lightning characteristics. The inset of Fig. 9 shows an extracted Phantom video frame during event UF 08-18. From the northerly view shown in Fig. 9 and an orthogonal westerly view, it is evident that the glowing region touched only a small section of the top electrode and that contact with that electrode took place after the luminous region separated from the stainless steel plates.

The full duration of the persistent glow around/above the stainless steel plates was approximately 648 ms. The distinct ball-shaped luminous glow was clearly separated from the stainless steel plates for approximately 266 ms. Interestingly, the only evidence of significant arcing damage to either stainless steel plate occurred on the bottom face of the bottom plate, a pitted area about 9 mm in diameter in the middle of the plate. When the arc discharge from the top electrode to the top plate was visible in the high-speed video, it appeared to contact the top plate on its northwest edge.

Fig. 8. Integrated video frames showing total luminosity from the silicon particle shower.

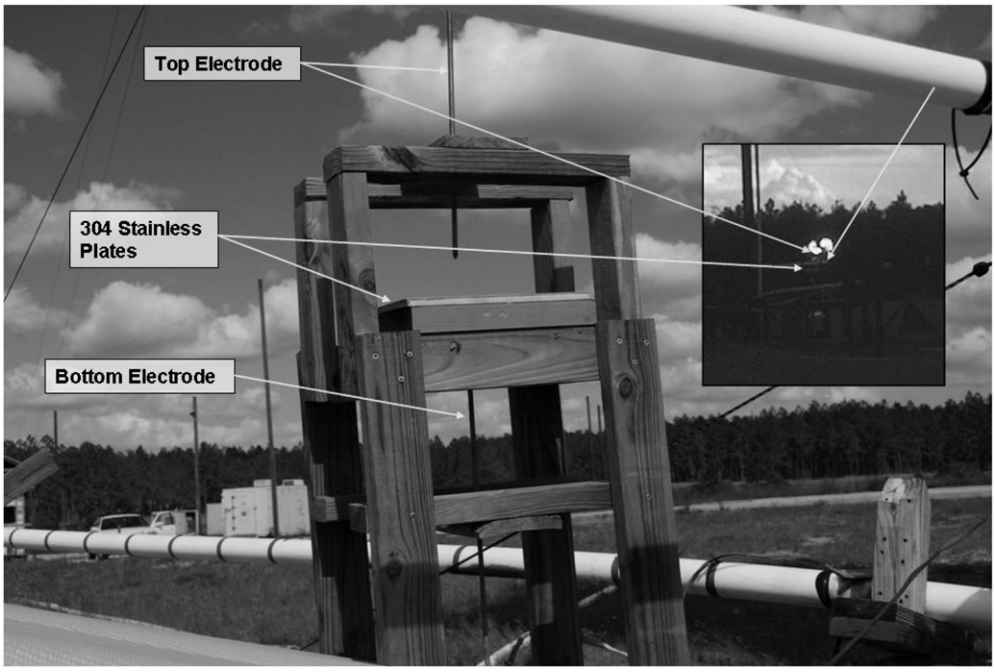

Fig. 9. Stainless steel plate experiment placed on the IS path to ground.

Fig. 10 shows twenty extracted Phantom video frames from the stainless steel plate experiment. The frames shown were taken at 16 ms intervals from just prior to the full separation of the glowing ball from the stainless plates, 328 ms after the first arc is seen on the stainless plates, to the point in time where all the glowing sections were extinguished, 648 ms following the initial arc on the stainless plates. In the images shown, the top glowing region is above the stainless steel plates. Fig. 10 also shows (in ten of the extracted Phantom video frames) the persistent glow on/above a pine tree trunk (time progressing from left to right, distance scales in units of meters), as discussed in B.2 below.

The IS duration of event UF 08-18 was approximately 300 ms with a charge transfer of about 7 C. The initial arc above the stainless plates was observed 45 ms prior to the complete ignition of the triggering wire. After the triggering wire exploded, a constant intense luminous glow was photographed, surrounding the stainless plates for 340 ms. This glow expanded to nearly a meter in diameter and is assumed to be the combination of multiple continuous arcs above and below the stainless plates. About 342 ms after the explosion of the triggering wire, the luminous glow receded and transitioned into a distinct oblong ball-shape form suspended approximately 30 cm above the top stainless steel plate. The initial ball was, at maximum, 71 cm in width and 48 cm in height when it was clearly detached from the plates, after about 32 ms in Fig. 10. Twenty-six milliseconds after the oblong glowing ball became clearly separated from the stainless plates, it split into two distinct round ball-shaped forms that shrunk in size with each subsequent frame. The two glowing balls appeared to remain relatively stationary; they did not appear to rise. When the balls became clearly split, the left ball was 43 cm wide and 33 cm high. The right ball was 33 cm wide and 33 cm high. The first return stroke occurred approximately 394 ms after the explosion of the triggering wire. Ideally, the intercepting wire over the top of the tower launcher would divert the entire return stroke current to the return stroke path to ground. However, during UF 08-18, a portion of the incident current due to the first four return strokes passed down the IS path to ground (the frames showing the return stroke luminosity are not presented in Fig. 10). However, the return strokes did not contribute to *any change* in luminosity or shape of the glowing region suspended above the plates. Around 18 ms after the first return stroke, the left glowing ball began to lose shape and split into two distinct sections. The top left ball was 20 cm in width and 13.5 cm in height, the bottom left ball was 33 cm in width and 20 cm in height, and the right ball was 33 cm in width and height. The second return stroke occurred 6 ms later. About 2 ms after the second return stroke, the glowing form above the plates split into four distinct sections, each with size ranging from 10 to 33 cm in width and 33 cm in height. The luminosity of each section declined uniformly with each subsequent frame. About 16 ms after the second return stroke, five distinct balls were visible, ranging in size from 10 to 20 cm. The third return stroke occurred 18 ms after the persistent glow split into five sections, but again, the arcs between the electrodes and the stainless plates due to the return stroke current did not effect the suspended glowing form above. All five sections declined steadily in luminosity until the top left ball extinguished 48 ms after the third return stroke. Twelve milliseconds later, the bottom left ball vanished, leaving three illuminated regions. The fourth return stroke occurred 2 ms after the fourth ball disappeared. About 40 ms after the fourth return stroke, the right-most glowing section extinguished, leaving two faintly illuminated regions. The fifth return stroke occurred 12 ms after the third glowing section disappeared and followed the RS path to ground. All of the four subsequent return stroke currents also followed the diverted (RS) path to ground from the intercepting wires. The bottom ball vanished about 10 ms after the fifth return stroke, and the remaining ball disappeared 30 ms later. Table 2 lists the peak currents and times for the first five return strokes relative to the full ignition of the triggering wire.

Although the bottom face of the bottom stainless steel plates is clearly marked by arcing, the top face of the top plate, which was wet with rain, showed no evident damage except for some small marks on the edges of the plate, although the glowing region appeared to have emanated from the top. While the composition

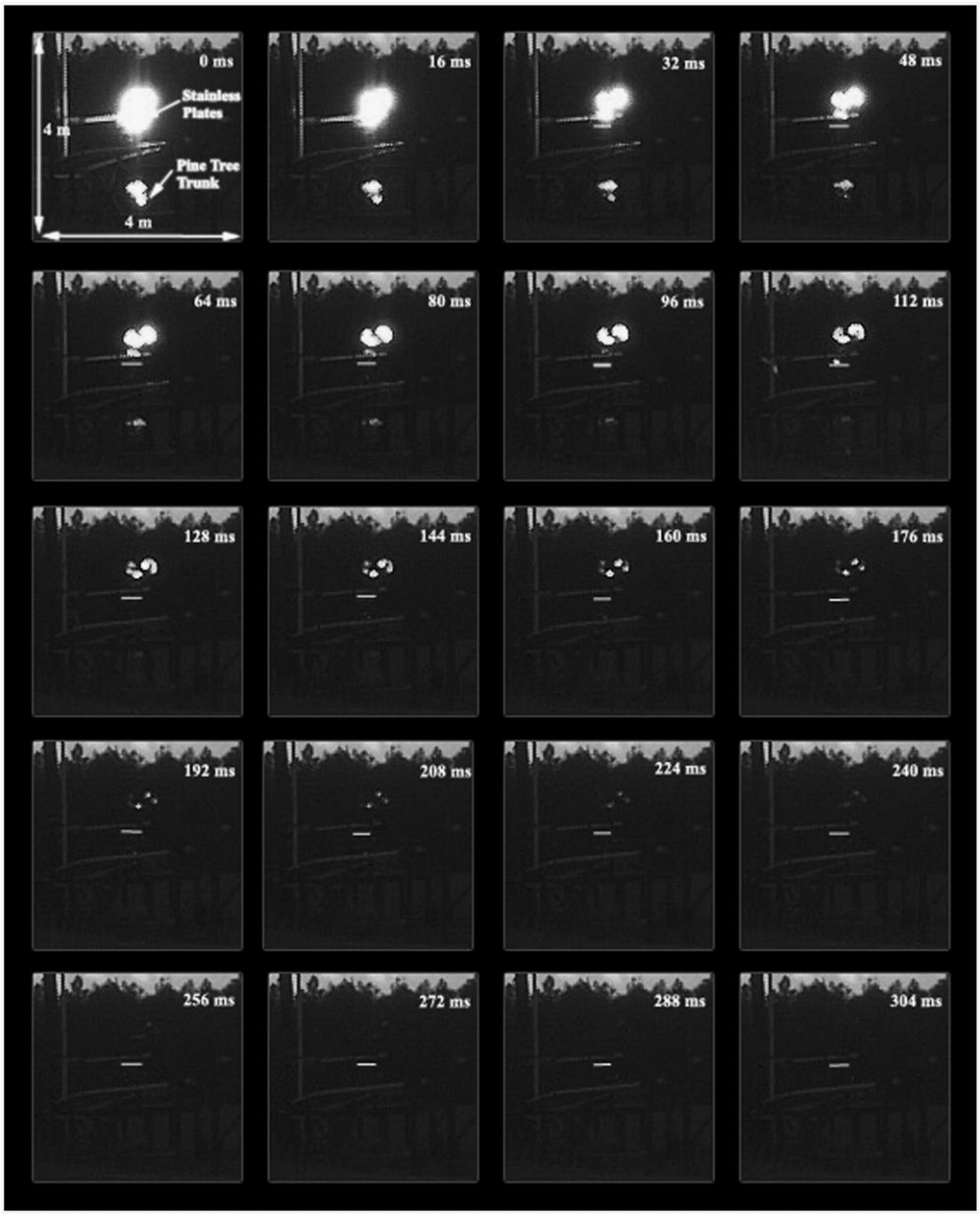

Fig. 10. Extracted Phantom video frames showing persistent illuminated regions on/above both the stainless steel plates (top glow) and the pine tree trunk (bottom glow) during UF 08-18. The white horizontal line marks the location of the top stainless steel plate.

Table 2
Peak current and return stroke times relative to the full ignition of the triggering wire for UF 08-18.

Stroke	Peak current (kA)	Time (ms)
1	11.6	394
2	9.2	418
3	20.8	452
4	16.2	514
5	7.6	566

of the resulting luminous ball is uncertain, the stainless steel plates, galvanized steel electrodes, water, and the surrounding wooden support frame may all have made some contribution to the observed luminous phenomenon.

Event B.2: A piece of braided wire connected the bottom metal rod electrode to a freshly cut section of pine tree trunk resting in the swimming pool filled with salt water and connected directly to the IS path to ground. A large galvanized nail was used to connect the braided wire to the cambium through the top of the pine tree trunk. A second piece of braided wire was connected to the cambium on the bottom side of the pine tree trunk by another galvanized nail and then clamped to the grounded ring electrode on the inner circumference of the swimming pool. The purpose of the nails was to force the incident current to pass through the pine tree trunk as opposed to arcing directly over the bark to the ring electrode. An identical experiment was present in the return stroke path to ground. During the IS process, the first glow on the top of the pine tree trunk occurred 4 ms after the initial glow on the stainless plates overhead and around 38 ms prior to the full explosion of the triggering wire. The illuminated region reached a maximum width of about 48 cm before completely separating from the top of the pine tree trunk 342 ms after the initial glow was recorded. The glowing region above the section of pine tree trunk appeared to rise slightly and declined in luminosity with

each subsequent frame. The smaller persistent glowing region directly on top of the pine tree trunk extinguished about 42 ms after the separation. The first return stroke occurred 90 ms after the glowing region separated from the top of the section of pine tree trunk. Similar to the stainless steel plates, the arcs around the pine tree trunk due to the return stroke current had no effect on the glowing region above the top of the tree trunk. The second return stroke occurred 24 ms later and also did not affect the remaining glowing region. After the second return stroke, the glowing region above the pine tree trunk section declined in luminosity and became disorganized. It finally disappeared around 28 ms after the second return stroke. The full duration of the glow on/above the pine tree trunk was approximately 484 ms, while the clearly separated glowing region survived for approximately 142 ms. No persistent glowing regions were recorded on/above the pine tree trunk placed in the RS path to ground. While the composition of the glowing region above the section of pine tree trunk is also uncertain, we expect that sap, water, electrode metal, and the wood itself may have all made contributions. The first frame in the image sequence of Fig. 10 shows the glowing region on the pine tree trunk just prior to separation. The following nine images show the glowing region gradually rising above the pine tree trunk section as it declined in size and luminosity. Phenomena similar to that described for the section of pine tree trunk above were recorded on four separate occasions (UF 08-11, UF 08-12, UF 08-13, UF 08-17), all during the IS process. In each case, the glowing regions extinguished within 350 ms.

4. Comparison of observations with theoretical behavior of decaying spheres of hot air

We measured the luminosity vs. time of the total luminous region in Fig. 10 starting at about 32 ms when the oblong luminous ball was clearly detached from the plate. The luminosity decayed essentially exponentially, a factor of about 3.5 in about 200 ms. The initial "diameter" of the oblong total ball luminosity is about 0.5 m. Lowke et al. (1969) calculate the flux density of visible light from a 0.4 m diameter sphere of air at initial temperature of 10,000 K (characteristic of an electric arc in air) as it decays. Several seconds are needed for the visible radiation to decrease an order of magnitude. It would appear that our luminosity decreases somewhat faster than the calculations of Lowke et al. (1969) indicate, likely because of an irregular initial temperature as a function of position within the luminosity above the stainless steel plates. That is, our luminous volume is actually a number of smaller luminous regions, evident as the overall luminosity decays. Lowke et al. (1969) state that the rate of decay of a central temperature of a uniform luminous ball of air is inversely proportional to its surface area (diameter squared). From the above, we might well conclude that the ball above the stainless steel plate is basically hot air with enough heavy material in its composition to maintain neutral buoyancy.

Related to the calculations of Lowke et al. (1969) for spheres of hot air are the calculations of Uman and Voshall (1968) for cylindrical regions of hot air approximating the decaying lightning channel after current cessation. Uman and Voshall (1968) suggest that bead lightning, a phenomenon in which the lightning channel decays into a sequence of visually luminous regions separated by non-luminous regions (see Rakov and Uman (2003) for a thorough review of bead lightning), could be caused by the luminous regions being of larger radius and hence decaying more slowly in temperature and luminosity. It is not out of the question that ball lightning and bead lightning are in some way related.

5. Comparison with laboratory ball lightning experiments

We have apparently duplicated, with uncontrolled currents from triggered lightning, two classes of laboratory experiments purported in the literature to represent ball lightning or some aspects of ball lightning. The first class of experiments, the experiments of Stephan and Massey (2008), following the initial work of Paiva et al. (2007), showed that electric arcs on silicon, aluminum, and copper could produce liquid metal spheres of 0.1–1.0 mm diameter that glow by surface combustion. These glowing balls may well represent one class of phenomena that has been described as ball lightning, as suggested by Stephan and Massey (2008). We show a similar if not identical phenomenon in Fig. 8, although our optical system resolution is such that the balls appear to be centimeter size. Stephan and Massey (2008) show that their silicon spheres have cores that are less than 1 mm in diameter when viewed through a welding filter, but appear to be centimeter size on normal photographs. They argue that the human observer would interpret the luminosity as considerably larger than it actually is; partly because of the cloud of particulates that surrounds the spheres in motion and partly via psychological impression. Our Fig. 8 shows a shower of glowing objects, whereas Stephan and Massey (2008) and Paiva et al. (2007) were able to produce both showers and single glowing spheres in the controlled laboratory environment. Perhaps we sometimes produced single spheres in striking metals, but those would have been difficult to detect with our experimental setup.

The second class of experiments, those producing flame-like phenomena above dirty water in which arcing occurs, is exemplified by the work of Versteegh et al. (2008) who used tap water and distilled water with salt additives. We produced flame-like phenomena of similar shape and duration above NaC1 salt water, as shown in Fig. 5. It is not clear that this phenomena, while interesting, has any direct relation to natural ball lightning, but it may.

6. Summary

During the triggered lightning/ball lightning experiment, about 100 different material samples were exposed to both relatively continuous (IS and inter-return-stroke continuing current) and to impulsive (RS) triggered lightning current. All events with properties in any way similar to those reported by eye-witness and laboratory accounts of ball lightning were produced by slowly varying, relatively low amplitude currents. No events with sustained luminosity duration greater than 100 ms were recorded as a result of impulsive return stroke currents. We do not claim to have produced ball lightning. The luminous phenomenon observed above the stainless steel plates as shown in Fig. 10 most closely resembled the accounts of ball lightning described in the literature in that it has a defined shape, did not rise appreciably, and had a duration that might be misinterpreted by an observer as a second or so, whereas it was actually less than 0.5 s. We apparently duplicated the laboratory experiments of Stephen and Massey (2008) and Paiva et al. (2007) who produced small combusting metal spheres from arcs to metals, a phenomenon that might represent one class of natural ball lightning observation, and of Versteegh et al. (2008) who produced a flame-like phenomenon via arcing in tap water and water containing salts such as calcium chloride, a phenomena that, along with the luminous phenomena produced above the tree sections struck by triggered lightning, may represent some component of the overall ball lightning phenomenon.

Acknowledgments

This research was supported in part by the U.S. Air Force Research Laboratory, Eglin Air Force Base, Florida, under the very helpful direction of J. Gregory Glenn. We also wish to thank the many researchers worldwide who provided useful suggestions regarding the experiment.

Appendix. List of samples tested

6/10/08: UF 08-02

Note: Material samples are listed according to their physical placement on the PVC pole. Samples are listed in order of decreasing height placement.

1. Brass #1—A 1/8 in brass rod with diameter of 3.18 mm implying 7.94 mm^2 cross-sectional area. The center necked down area is 2×2 mm^2 with a 4 mm^2 cross-sectional area.
2. Copper #2—A #10 copper wire with a diameter of 2.57 mm and cross-sectional area of 5.2 mm^2. The center necked down area is 1.4×1.4 mm^2 with cross-sectional area of 1.96 mm^2.
3. Aluminum #1—Aluminum wire with a diameter of 4.46 mm and cross-sectional area of 15.6 mm^2. The necked down section has dimensions 3×3 mm^2 (9 mm^2 cross-sectional area) and is 4 mm long.
4. Copper #1—A #10 copper wire with a diameter of 2.57 mm and cross-sectional area of 5.2 mm^2. The necked down section has dimensions 1.8×1.8 mm^2 with a 3.24 mm^2 cross-sectional area.
5. Aluminum #2—Aluminum wire with a diameter of 3.4 mm (3.08 mm^2 area). The necked down section has dimensions 2×2 mm^2 with a 4 mm^2 cross-sectional area.
6. Aluminum Plate #1—Aluminum plate that is 1.52 mm thick with dimensions of 11.4×17.8 cm^2. Electrical connection is made on one side via #10 AWG stranded wire connected to 2 existing holes. Electrode on other side made from 6 cm to 20 thread pointed steel rod with a gap of 5 cm.
7. Silicon #1—Silicon wafer that is .635 mm thick. The wafer has height of 9.5 cm and length 14.6 cm. Electrodes are .6 cm threaded steel rods on each side of the wafer located 5.6 cm from flat side and 3 cm above bottom. 10 cm PVC pipe ring added for support on the wafer.
8. Silicon #2—One half of a full disk with 6 cm threaded steel rod electrodes located on each side of the silicon surface with a gap of 6 cm. 10 cm PVC pipe rings support both sides.
9. Pool—45 gallons of water at 5 g sodium chloride (salt) per gallon, totaling 225 g of sodium chloride. The ring electrode is around the edge of the pool 2.5 cm below water level. There are two grounding rods, one on each side of the pool. The lightning current electrode comes down into the pool an inch below the surface of the water in the center of the pool.

6/29/08: UF 08-04

Note: Material samples are listed according to their physical placement on each PVC pole. Samples are listed in order of decreasing height placement.

ICC pole

1. Silicon #3—Solid attachment to the dull side of silicon wafer with a 5 cm gap on the mirrored side.
2. Copper Powder #1—Two grams of dry, spherical, −100 mesh, 99.5% metals basis of copper powder in PVC container.
3. Aluminum Plate #2—Six centimeters thick piece of aluminum cut from a 5 cm aluminum angle. There is a 2.5 cm gap to a steel bolt electrode.
4. Copper #2—A #10 AWG copper wire with a diameter of 2.57 mm. The necked down portion of the copper wire has dimensions 1.4×1.4 mm^2 for a cross-sectional area of 1.96 mm^2.
5. Copper #3—A #14 AWG copper wire with a necked down portion in the middle of the sample. The copper wire has a diameter of 1.6 mm, while the necked down portion has a diameter of 8 mm and respective cross-sectional area of 1.04 mm^2.
6. Copper #4—A 1.11 mm diameter copper wire with a necked down portion of diameter 0.55 mm. It has a cross-sectional area of 0.48 mm^2.
7. Brass #2—A 1.58 mm diameter #14 AWG brass wire with a necked down portion of diameter 0.79 mm. It has a necked down cross-sectional area of 0.98 mm^2.
8. Silicon Powder #1—One gram of dry, crystalline, −325 mesh, 99.5% metals basis silicon powder in a PVC container.
9. Unknown MSE Sample #1—Unknown sample in tube from Materials Science Engineering Department.
10. Pool—Water filled pool with a ratio of 10 g NaCl per gallon of H_2O.

Return stroke pole

1. Silicon #4—A solid attachment is made to the dull side of silicon wafer with a 5 cm gap on the mirrored side.
2. Aluminum Powder #1—One gram of dry, spherical, APS 10.0–14.0 μm, 98% metals basis aluminum powder in PVC container.
3. Aluminum Plate #3—Aluminum plate with dimensions 11.4 cm by 17.8 cm. Electrical connection on one side via #10 AWG stranded wire connected to 2 existing holes. Electrode on opposite side made from 6 cm to 20 thread pointed steel rod with a 5 cm gap.
4. KNO_3 and Silicon Powder #1—One gram each of KNO_3 and silicon powder for a total of 2 g inside a PVC container.
5. Sulfur and Silicon Powder #1—One gram each of sulfur and silicon powder for a total of 2 g inside of a PVC container.
6. Bat Guano #1—Roughly 2 g of bat guano in a PVC container.
7. Aluminum Wet Powder #1—One gram of aluminum powder with the same specifications as dry aluminum powder in a PVC container. Two milliliters of H_2O is added to the sample to provide moisture.
8. Copper Wet Powder #1—Two grams of copper powder with the same specifications as copper powder #1. Two milliliters of H_2O is added to the sample to provide moisture.
9. Pool—Water filled pool with a ratio of 10 g NaCl per gallon of H_2O.

06/30/08: UF 08-08

Note: Material samples are listed according to their physical placement on each PVC pole. Samples are listed in order of decreasing height placement.

ICC pole

1. Silicon #3—Solid attachment to the dull side of silicon wafer with a 5 cm gap on the mirrored side.
2. Copper Powder #1—Two grams of dry, spherical, −100 mesh, 99.5% metals basis of copper powder in PVC container.
3. Aluminum Plate #2—A .6 cm thick piece of aluminum cut from a 5 cm aluminum angle. There is a 2.5 cm gap to a steel bolt electrode.
4. Copper #2—A #10 AWG copper wire with a diameter of 2.57 mm. The necked down portion of the copper wire has dimensions 1.4×1.4 mm^2 for a cross-sectional area of 1.96 mm^2.

5. Copper #3—A #14 AWG copper wire with a necked down portion in the middle of the sample. The copper wire has a diameter of 1.6 mm, while the necked down portion has a diameter of .8 mm and respective cross-sectional area of 1.04 mm^2.
6. Copper #4—A 1.11 mm diameter copper wire with a necked down portion of diameter 0.55 mm. It has a cross-sectional area of 0.48 mm^2.
7. Brass #2—A #14 AWG brass wire (1.58 mm diameter) with a necked down portion of diameter 0.79 mm. It has a necked down cross-sectional area of 0.98 mm^2.
8. Silicon Powder #1—One gram of dry, Crystalline, -325 mesh, 99.5% metals basis silicon powder in a PVC container.
9. Unknown MSE Sample #1—Unknown sample in tube from Materials Science Engineering Department.
10. Pool—Water filled pool with a ratio of 10 g NaCl per gallon of H_2O.

Return stroke pole

1. Silicon #4—A solid attachment is made to the dull side of silicon wafer with a 5 cm gap on the mirrored side.
2. Aluminum Powder #1—One gram of dry, spherical, APS 10.0–14.0 micron, 98% metals basis aluminum powder in PVC container.
3. Aluminum Plate #3—Aluminum plate with dimensions 11.4 cm by 17.8 cm. Electrical connection on one side via #10 AWG stranded wire connected to 2 existing holes. Electrode on opposite side made from .6 cm-20 thread pointed steel rod with a 5 cm gap.
4. KNO_3 and Silicon Powder #1—One gram each of KNO_3 and silicon powder for a total of 2 g inside a PVC container.
5. Sulfur and Silicon Powder #1—One gram each of sulfur and silicon powder for a total of 2 g inside of a PVC container.
6. Bat Guano #1—Roughly 2 g of bat guano in a PVC container.
7. Aluminum Wet Powder #1—One gram of aluminum powder with the same specifications as dry aluminum powder in a PVC container. Two milliliters of H_2O is added to the sample to provide moisture.
8. Copper Wet Powder #1—Two grams of copper powder with the same specifications as copper powder #1. Two milliliters of H_2O is added to the sample to provide moisture.
9. Pool—Water filled pool with a ratio of 10 g NaCl per gallon of H_2O.

07/12/08: UF 08-11

Note: Material samples are listed according to their physical placement on each PVC pole. Samples are listed in order of decreasing height placement.

ICC pole

1. 5 g powder carbon—2.5 g powder carbon in a PVC container.
2. Bat guano and SiO_2—Bat guano mixed with SiO_2 in a PVC container.
3. Copper #2—A #10 AWG copper wire with a diameter of 2.57 mm. The necked down portion of the copper wire has dimensions 1.4×1.4 mm^2 for a cross-sectional area of 1.96 mm^2.
4. Copper #3—A #14 AWG copper wire with a necked down portion in the middle of the sample. The copper wire has a diameter of 1.6 mm, while the necked down portion has a diameter of .8 mm and respective cross-sectional area of 1.04 mm^2.
5. Copper #4—A 1.11 mm diameter copper wire with a necked down portion of diameter 0.55 mm. It has a cross-sectional area of 0.48 mm^2.
6. Brass #2—A #14 AWG brass wire (1.58 mm diameter) with a necked down portion of diameter 0.79 mm. It has a necked down cross-sectional area of 0.98 mm^2.
7. Pool #1—Pool filled with 10 g NaCl per gallon of water. The electrode is made from connecting the shield braid into the center section of a tree roughly a foot in length.

Return stroke pole

1. 5 g powder carbon—2.5 g powder carbon in a PVC container.
2. Bat guano and SiO_2—Bat guano mixed with SiO_2 in a PVC container.
3. Pool #2—Pool filled with 10 g NaCl per gallon of water. The electrode is made from connecting the shield braid into the center section of a tree roughly 15 cm in length.

07/23/08: UF 08-12

Note: Material samples are listed according to their physical placement on each PVC pole. Samples are listed in order of decreasing height placement.

ICC Pole

1. Stainless steel plates—Located on launch tower level 3.
2. 5 g wet powdered carbon—Suspended PVC container
3. $Sn+Ag_2S+Ag+H_2O$—Suspended PVC container
4. Bat guano+powdered carbon—Suspended PVC container
5. Copper #2 (#10 AWG)—Notch of .6 mm
6. Copper #3 (#14 AWG)—Notch of .38 mm
7. Copper #4 (#18 AWG)—Notch of .43 mm
8. Brass #2 (#14 AWG)—Notch .43 mm
9. Brass #3 (#14 AWG)—Notch .56 mm
10. Copper #5 (#28 AWG)
11. Copper #6 (#22 AWG)
12. Pool #1—Pool filled with 10 g NaCl per gallon of water. The electrode is made from connecting the shield braid into the center section of a tree roughly a foot in length.

Return stroke pole

1. 5 g wet powdered carbon—Suspended PVC container
2. $Sn+Ag_2S+Ag+H_2O$—Suspended PVC container
3. Bat guano+powdered carbon—Suspended PVC container
4. Pool #2—Pool filled with 10 g NaCl per gallon of water. The electrode is made from connecting the shield braid into the center section of a tree roughly a foot in length.

07/27/08: UF 08-13

Note: Material samples are listed according to their physical placement on each PVC pole. Samples are listed in order of decreasing height placement.

ICC pole

1. Stainless steel plates—Located on launch tower level 3.
2. 5 g wet powdered carbon—Suspended PVC container
3. $Sn+Ag_2S+Ag+H_2O$—Suspended PVC container
4. Bat guano+powdered carbon—Suspended PVC container
5. Copper #2 (#10 AWG)—Notch of .6 mm
6. Copper #3 (#14 AWG)—Notch of .38 mm
7. Copper #4 (#18 AWG)—Notch of .43 mm
8. Brass #2 (#14 AWG)—Notch of .43 mm
9. Brass #3 (#14 AWG)—Notch of .56 mm
10. Copper #5 (#28 AWG)
11. Copper #6 (#22 AWG)
12. Pool #1—Pool filled with 10 g NaCl per gallon of water. The electrode is made from connecting the shield braid into the center section of a tree roughly 30 cm in length.

Return stroke pole

1. 5 g wet powdered carbon—Suspended PVC container
2. $Sn+Ag_2S+Ag+H_2O$—Suspended PVC container
3. Bat guano+powdered carbon—Suspended PVC container
4. Pool #2—Pool filled with 10 g NaCl per gallon of water. The electrode is made from connecting the shield braid into the center section of a tree roughly 30 cm in length.

09/11/08: UF 08-17

Note: Material samples are listed according to their physical placement on each PVC pole. Samples are listed in order of decreasing height placement.

ICC Pole

1. 5 g wet powdered carbon—Suspended PVC container
2. $Sn+Ag_2S+Ag+H_2O$—Suspended PVC container
3. Bat guano+powdered carbon—Suspended PVC container
4. Copper #2 (#10 AWG)—A notch of .6 mm
5. Copper #3 (#14 AWG)—A notch of .38 mm
6. Copper #4 (#18 AWG)—A notch of .43 mm
7. Brass #2 (#14 AWG)—A notch .43 mm
8. Brass #3 (#14 AWG)—A notch .56 mm
9. Copper #5 (#28 AWG)
10. Copper #6 (#22 AWG)
11. Stainless steel plates
12. Pool #1—Pool filled with 10 g NaCl per gallon of water. The electrode is made from connecting the shield braid into the center section of a tree roughly 30 cm in length.

Return stroke pole

1. 5 g wet powdered carbon—Suspended PVC container
2. $Sn+Ag_2S+Ag+H_2O$—Suspended PVC container
3. Bat guano+powdered carbon—Suspended PVC container
4. Deuterium water
5. Pool #2—Pool filled with 10 g NaCl per gallon of water. The electrode is made from connecting the shield braid into the center section of a tree roughly 30 cm in length.

09/17/08: UF 08-18

Note: Material samples are listed according to their physical placement on each PVC pole. Samples are listed in order of decreasing height placement.

ICC pole

1. Stainless steel plates
2. Pool #1—Pool filled with 10 g NaCl per gallon of water. The electrode is made from connecting the shield braid into the center section of a tree roughly 30 cm in length.

Return stroke pole

1. Pool #2—Pool filled with 10 g NaCl per gallon of water. The electrode is made from connecting the shield braid into the center section of a tree roughly 30 cm in length.

References

Abrahamson, J., Dinnis, J., 2000. Ball lightning caused by oxidation of nanoparticle networks from normal lightning strikes on soil. Nature 403, 519–521.

Abrahamson, J., 2002. Ball lightning from atmospheric discharges via metal nanosphere oxidation: from soils, wood or metals. Philosophical Transactions: Mathematical, Physical and Engineering Sciences 360, 61–88.

Hu, J., Tsai, H.L., 2006. Effects of current on droplet generation and arc plasma in gas metal arc welding. Journal of Applied Physics 100, 053304.

Lowke, J.J., Uman, M.A., Liebermann, R.W., 1969. Toward a theory of ball lightning. Journal of Geophysical Research 74, 6887–6898.

Paiva, G.S., Pavão, A.C., de Vasconcelos, E.A., Mendes Jr., O., da Silva Jr., E.F., 2007. Production of ball-lightning-like luminous balls by electrical discharge in silicon. Physical Review Letters 98, 048501.

Rakov, V., 1999. Lightning discharges triggered using rocket-and-wire techniques. Recent Research Developments in Geophysics 2, 141–171.

Rakov, V., Uman, M.A., 2003. Lightning: Physics and Effects. Cambridge University Press, Cambridge.

Stenhoff, M., 1999. Ball Lightning: Unsolved Problem in Atmospheric Physics. Kluwer Academic and Plenum Publishers, New York (349 pp).

Stephan, K., Massey, N., 2008. Burning molten metallic spheres: one class of ball lightning? Journal of Atmospheric and Solar–Terrestrial Physics 70 1589–1596.

Uman, M.A., Voshall, R.E., 1968. Time interval between lightning strokes and the initiation of dart leaders. Journal of Geophysical Research 73, 497–506.

Uman, M.A., Rakov, V.A., Rambo, K.J., Vaught, T.W., Fernandez, M.I., Cordier, D.J., Chandler, R.M., Bernstein, R., Golden, C., 1997. Triggered-lightning experiments at camp blanding, Florida (1993–1995). Transactions of the IEE Japan 117-B, 446–452.

Versteegh, A., Behringer, K., Fantz, U., Fussmann, G., Jüttner, B., Noack, S., 2008. Long-living plasmoids from an atmospheric water discharge. Plasma Sources Science and Technology 17, 024014.